Electronic Supplementary Information (ESI) for:

A Low Temperature Iron Molten Air Battery

Baochen Cui[a,] and Stuart Licht[*,a]

ESI contains:

1) Molten Air mechanism of action (reproduced in part, reproduced with permission from S. Licht, B. Cui, J. Stuart, B. Wang and J. Lau[a], *Energy & Environmental Science*, 2013, **6,** 3646.**)**

2) Electrochemistry of iron in molten carbonates (reproduced with permission from S. Licht, H. Wu, Z. Zhang and H. Ayub, *Chem. Comm.,* 2011, **47,** 3081.)

1) Molten Air mechanism of action:

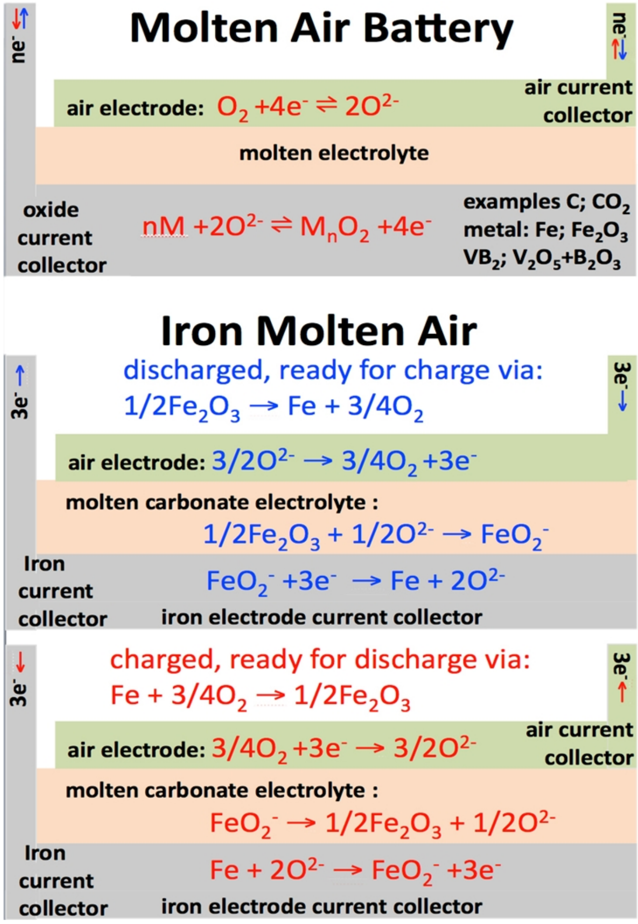

Scheme 1-ESI Top: The molten air battery. Bottom: The iron molten air battery; illustration of the charge/discharge in molten carbonate. The charging or discharging process is indicated by red or blue text & arrows.

Recently rechargeable molten air batteries are introduced, and several examples of their battery chemistry demonstrated.[1] Unlike prior rechargeable molten batteries, the battery is not burdened by the weight of the active chargeable cathode material. The rechargeable molten air electrode instead uses oxygen directly from the air to yield high battery capacity. This electrode was shown to be compatible with several high capacity multiple electron redox couples. Three demonstrated new batteries chemistries are the metal (iron), carbon and VB_2 molten air batteries.

Other classes of molten electrolyte batteries had been investigated. A molten sulfur battery has been widely studied, particularly for electric car and grid applications.[13-16] During discharge, the battery uses sulfur and sodium (or potassium) for the respective cathode and anode storage materials, and these high temperature molten components are kept from chemically reacting by a solid electrolyte beta alumina separator. Both the molten[13-16] and room temperature class of sulfur cathode batteries,[17,18] are limited by the maximum intrinsic capacity of the 2 electron per sulfur (2 Faraday/ 32g sulfur), while the new Molten Air batteries are independent of this mass limitation.

Internal combustion engines driven by gasoline (petrol) typically reach temperatures of 700°C, higher temperatures occur within the manifold and at the catalytic converter. Internal combustion engines driven by diesel typically reach temperatures of 600°C or higher. Here we study Molten Air Batteries that can operate at temperatures $\leq$ 600°C and demonstrate this aspect of EV (electric vehicle) compatibility. Molten Air electrochemical energy storage with is represented in Scheme 1-ESI in both generalized form and with a specific example (the Iron Molten Air battery). As illustrated for the Iron Molten Air example, during charging, iron oxide is converted to iron metal via a three-electron reduction, and O_2 is released to the air. During discharge iron metal is converted back to iron oxide.

To date, Molten Air Battery chemistries were demonstrated using anodes discharging (i) the $11e^-$ oxidation of VB_2 (with a vanadate/borate electrolyte), (ii) the $4e^-$ Carbon or (iii) the $3e^-$ Iron (each with carbonate electrolyte). Each only at temperatures of 730°C or higher.[1] Lower temperature battery chemistries would greatly expedite their utility for electric vehicle applications. In this study we probe one example, Iron Molten Air, which includes a lower temperature battery chemistry.

Table 1. The charged intrinsic energy storage capacity of various molten air rechargeable batteries. Volumetric energy capacity, E_{vol}, is calculated from the number of electrons stored, n, the density d, the Faraday constant, F = 26.80 Ah mol^{-1}, the formula weight, FW, and E° in accord with Eqs. 1, 2 or 3 as E_{vol} = ndE°F / FW. The cell potential at unit activity, E°, is temperature dependent. For example, while constant over a wide temperature range at 1.0 V for the carbon anode, E° decreases for the iron anode from 1.2 to 0.9 V with temperature increase from 25°C to 850°C.[21] The theoretical storage capacity of air batteries is traditionally calculated based on the mass or volume of the reduced active anode material (such as zinc in a zinc air battery) as oxygen is freely available from the air. However, in practice the mass and volume of air battery systems increases with the uptake of oxygen during discharge, and the limiting capacities may be better represented by a form half way between the charged and discharged state. Hence, the final mass, volume and capacity of lithium air batteries need to include the oxygen to form the oxidized product, Li_2O. This effect is large for lithium air batteries as a mole of Li increases from 6.9g to a discharged mass of 14.9g ($1/2Li_2O$)), and relatively less for iron which increases from a molar mass of 55.8 g to a discharged mass of 79.8g ($1/2Fe_2O_3$). Table 1 calculates air battery capacities in the traditional manner, but we note that this provides only an upper limit to the capacity of such air batteries when fully charged.

Anode	Formula Weight kg mol^{-1}	e^-s stored	Charge Capacity Ah/kg	d, kg l^{-1}	E°, V vs O_2	Energy Capacity gravimetric Wh kg^{-1}	Energy Capacity volumetric Wh liter^{-1}
Iron	0.05585	$3e^-$	1,440	7.2	1.0	1,400	10,000
Carbon	0.01201	$4e^-$	8,930	2.1	1.0	8,900	19,000
VB_2	0.07256	$11e^-$	4,060	5.1	1.3	5,300	27,000

The right column of Table 1 compares the intrinsic capacity of these batteries, which is *one to two orders of magnitude greater* than that of the volumetric energy capacity of conventional Li ion batteries. Lithium (metal) air also has a lower volumetric energy capacity. While Li's gravimetric charge capacity (3860 Ah/kg) is similar to that of VB_2 (4,060 Ah/kg), it has a lower 6,200 Wh liter^{-1} volumetric capacity due to a low density (0.534 kg liter^{-1}), and single, rather than multiple, electron charge transfer.

Accelerated testing of the VB_2 or Carbon molten air batteries presents fundamental challenges avoided by the Iron Molten Air Battery. In each case of the three cases the storage capacity is high, and it is a challenge to limit the storage reactant availability. Constraining the high intrinsic capacity of the VB_2 molten air cell requires thin cross sections of electrolyte to limit the high capacity, which is an interesting, but longer-term challenge. In the VB_2 Molten Air Battery the reactant is comprised from (and not added to) a molten vanadate and borate electrolyte and are charged to form the VB_2 storage product:

VB_2 molten air battery, 11e$^-$: $VB_2 + 11/4O_2 \rightleftharpoons B_2O_3 + V_2O_5$ (1)

The Carbon Molten Air Battery provides the greatest challenge to constrain its high capacity for accelerated testing purposes. The battery reactant is formed via the molten carbonate electrolyte from air borne CO_2. In the presence of CO_2, the electrolyte need not be consumed during discharge. This cell uses only atmospheric oxygen and atmospheric CO_2 during cycling (while one of the mobile ions during charge cycling is electrolytic carbonate, carbonate involved in the individual electrode reactions balances out in the global reaction). The mass of the electroactive storage materials are "free (or zero)" in the context of the conventional battery energy density calculation, in that they are available in the air and are not carried within, or stored externally, to the battery. This is evident by comparing the mechanism when the cell is charged and discharged in either the absence, or presence of CO_2. While many carbonates are available, for clarity, a single carbonate (lithium carbonate) is used in the mechanism below:

global 4e- Carbon Molten Air charge/discharge:

$CO_2 \rightleftharpoons C + O_2$ (2)

CO_2 dissolution into electrolyte: $Li_2O + CO_2 \rightarrow Li_2CO_3$ (2a)

4e$^-$ battery cycling $Li_2CO_3 \rightleftharpoons C + Li_2O + O_2$ (2b)

In a manner analogous to the VB_2 molten air cell, in the absence of atmospheric CO_2 the Carbon Molten Air Battery capacity is limited by the electrolyte. Constraining the high intrinsic capacity of this carbonate molten air cell also requires thin cross sections of electrolyte to limit the high capacity, which is an interesting, but longer-term challenge. Without external CO_2 the Carbon Molten Air Battery capacity is limited by the carbonate electrolyte, such as lithium carbonate:

global 4e$^-$, carbonate limited, Carbon Molten Air charge/discharge:

$Li_2CO_3 \rightleftharpoons C + Li_2O + O_2$ (3)

Unlike the challenges to study of the Carbon or VB_2 Molten Air Batteries by constraining their intrinsic capacity, the capacity of an Iron Molten Air Battery can be controlled by limiting the iron added to the cell. As one example of the recently introduced molten air battery class, we probe here the rechargeable nature of the Iron Molten Air Battery. Of the three examples of molten air batteries provided to date,[1] the Iron Molten Air example provides the easiest route to purposely restrict the battery capacity by limiting the iron reactant (by allowing free flow entry of air, but by constraining the concentration of dissolved iron salt in the electrolyte). We will probe sustainable current densities and discharge efficacy, and then demonstrate a pathway to lower temperature rechargeable Iron Molten Air batteries. The Iron Molten Air battery is represented by Eq. 4, and is facilitated by the Eq. 4a dissolution of Fe_2O_3 with Li_2O to form lithiated iron oxide, $LiFeO_2$,[5] followed by quasi-reversible charge/discharge of $LiFeO_2$ to iron, Eq 4b.

global 3e$^-$ Iron Molten Air charge/discharge:

$1/2Fe_2O_3 \rightleftharpoons Fe + 3/4O_2$ (4)

molten dissolution: $1/2Fe_2O_3 + 1/2Li_2O \rightleftharpoons LiFeO_2$

(4a)

3e$^-$ cycling: $LiFeO_2 \rightleftharpoons Fe + 1/2Li_2O + 3/4O_2$ (4b)

As elaborated on in section 3 (Temperature effects on thermodynamics & voltage of iron in molten carbonates), lithiated ferric iron oxides are extremely soluble in lithium ion containing carbonates. For example, 14 m (m is molal = mols solute / kg solvent) Fe(III) can dissolve in Li_2CO_3.[5,7] For the Iron Molten Air Battery, even higher amounts of iron are available for storage by maintaining a buffer of solid Fe_2O_3. This becomes soluble when existing dissolved Fe(III) is reduced to iron metal during the battery charging. This provides unusually high battery storage capacities.

The intrinsic volumetric energy capacity of the Iron Molten Air Battery, E_{vol}, is calculated from, n, the 3 electrons stored in the reduction to iron, the iron density d=7.2 kg/ l^{-1}, the Faraday constant, F = 26.80 Ah mol^{-1}, the formula weight, FW=0.05585 kg mol^{-1}. As Q=nF / FW this to gives a charge capacity of 1,440 Ah kg^{-1}, and based on an observed open circuit potential of E°=1.2V, yields a gravimetric energy capacity of E_{grav} = QE° and a volumetric energy capacity of E_{vol} = dQE this gives a gravimetric energy capacity of 1,728 Wh kg^{-1}, and a volumetric capacity of 12,0000 Wh liter^{-1}. This is *one to two orders of magnitude greater* than the volumetric energy capacity of conventional Li ion batteries. The theoretical storage capacity of air batteries is traditionally calculated based on the mass or volume of the reduced active anode material (such as zinc in a zinc air battery) as oxygen is freely available from the air. However, in practice the mass and volume of air battery systems increases with the uptake of oxygen during discharge, and the limiting capacities may be better represented by a form half way between the charged and discharged state. Hence for example if we were to consider a lithium air battery, the final mass, volume and capacity of these batteries need to include the oxygen to form the oxidized product, Li_2O. This effect is large for lithium air batteries as a mole of Li increases from 6.9g to a discharged mass of 14.9g (1/2Li_2O)), and relatively less for iron which increases from a molar mass of 55.8 g to a discharged mass of 79.8g (1/2Fe_2O_3).

We observe that Li_2CO_3, which melts at 723°C, and lower melting carbonate eutectics are effective electrolytes. Simple steel foil cathodes and nickel foil anodes are effective for either iron oxide[14-18] or carbon dioxide splitting. In addition to nickel, the nickel alloy inconel can simultaneously act as the air electrode and cell container. These anodes and cathodes can sustain high splitting (mA to A per cm^{-2}) current densities at low overpotential in molten lithium carbonate. These electrolyses for either iron oxide[1,6,7,12,19] or carbon dioxide splitting[1,20-21] can also represent charging of a molten air at high current density and low potential.

2) Electrochemistry of iron in molten carbonates

In the electrolyte Fe(III) originates from dissolved ferric oxides, such as $LiFeO_2$ or $LiFe_5O_8$. The potential for the three electron reduction to iron varies in accord with the general Nerstian expression, for a concentration [Fe(III)], at activity coefficient, α:

$$E_{Fe(III/0)} = E°_{Fe(III/0)} + (RT/nF)\log(\alpha_{Fe(III)}[Fe(III)])^{1/3} \quad \text{(S-4)}$$

Fig. 1-ESI summarizes the thermochemical calculated potentials constraining iron production in molten carbonate. The decrease in electrolysis potential with increasing Fe(III) varies as 6.6x10^{-5}VxT(electrolysis,K)/K (=RT/nF), which is accentuated by high temperature. Hence, from the thermodynamic perspective with a simple assumption of unit activity coefficient, a 14 molal iron concentration will decrease the 1223 K (950°C) electrolysis potential by a further 0.1 V. Higher activity coefficient, $\alpha_{Fe(III)} > 1$, would further decrease the thermodynamic potential to produce iron. In various concentrated electrolytes, activity coefficients, α, an order of magnitude, or more, higher than unity have been observed.

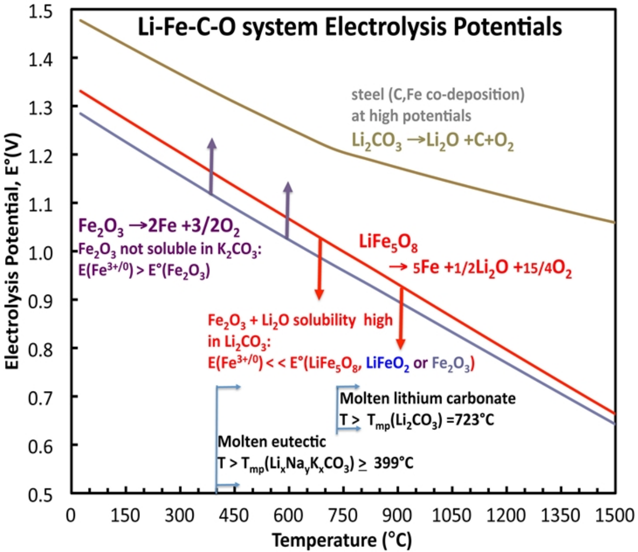

Fig. 1-ESI. The calculated electrolysis potentials of $LiFe_5O_8$, Fe_2O_3 or Li_2CO_3 at unit activity from the thermochemical data.[9,10] Vertical arrows indicate Nernstian shifts at high or low Fe(III) solubilities. ΔG(T) are better described for $LiFe_5O_8$ compared to $LiFeO_2$; hence as indicated, $LiFe_5O_8$ calculations are included in the figure.

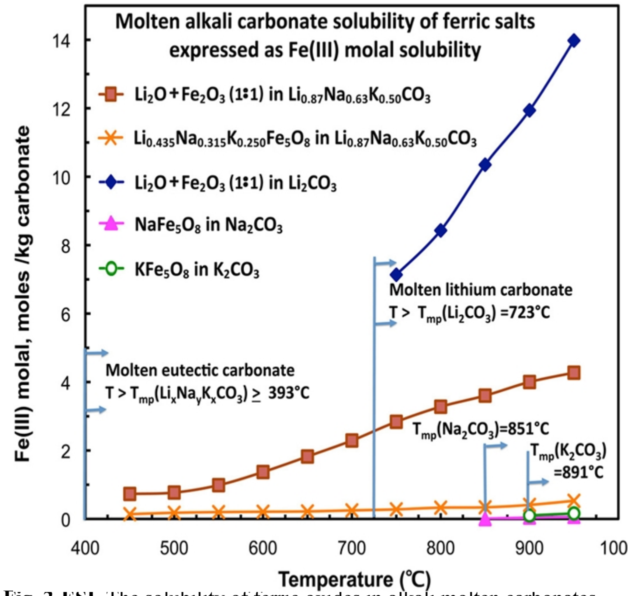

Fig. 2-ESI. The solubility of ferric oxides in alkali molten carbonates.

Fig. 2-ESI, presents the wide solubility variation of Fe(III) in different alkali carbonates, Fe(III) is not soluble up to over 950°C in either molten Na_2CO_3 or K_2CO_3. The addition of a 1:1 equivalent ratio of Li_2O to Fe_2O_3 dissolves in Li_2CO_3 without the reactive formation of CO_2, as $LiFeO_2$. As seen, the solubility of this Fe(III) dissolved as $LiFeO_2$ (by the addition of Li_2O + Fe_2O_3) in the alkali carbonate eutectic, $Li_{0.87}Na_{0.63}K_{0.50}CO_3$, is high, and at 750°C approaches half the solubility of the high solubility in the pure lithium carbonate electrolyte. The eutectic has the distinction of a greater molten temperature range (extending several hundred degrees lower than the pure lithium system). Solubility of this lithiated ferric oxide in the $Li_xNa_yK_zCO_3$ mixes provides an alternative molten media for the iron molten air battery, which compared to pure lithium carbonate, has the disadvantage of lower conductivity, but the advantage of even greater availability, and a wider operating temperature domain.

Also evident in Fig. 2-ESI, while the solubility of the lithiated ferric oxide in the eutectic carbonate is high, the solubility of a mixed alkali penta-iron octa-oxide salt, synthesized as $Li_{0.435}Na_{0.315}K_{0.250}Fe_5O_8$, is low, reaching a maximum concentration of only 0.5 m Fe(III) at 950°C.

The measured electrolysis (charging) potential is presented in Figure 3-ESI for dissolved Fe(III) in molten lithium carbonate. As seen, the charging potential increases with i) decreasing temperature, (ii) decreasing concentration of dissolved Fe(III), and (iii) an increasing charge density. As expected at low (< 0.A cm^{-2}) charge density, the measured potentials in the figure are considerably less than the room temperature 1.3V thermodynamic potential required to convert Fe_2O_3 to iron and oxygen.

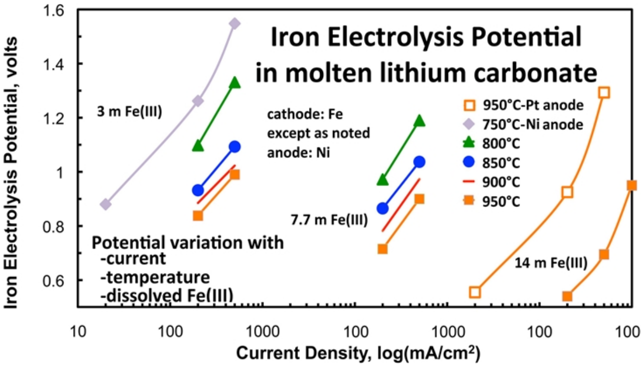

Fig. 3-ESI. The measured electrolysis potentials of iron, for dissolved Fe(III) in molten Li_2CO_3, as a function of the electrolyte temperature and the concentration of dissolved iron. The cell electrolysis potentials are measured as a function of constant current, with current density constrained by the cathode surface area.

Additional references

13. B. Dunn, H. Kamath and J. M. Tarascon, J. M. Electrical Energy Storage for the Grid: A Battery of Choices. *Science,* 2011, **334**, 9280935.
14. J. B. Goodenough, Rechargeable batteries: challenges old and new, *J. Solid State Electrochem.,* 2012, **16**, 2019.

15. K. B. Hueso, M. Armand and T. Rojo, *Energy Environ. Sci.,* 2013, **6**, 734.
16. X. Lu, B. W. Kirby, G. Li, J. Y. Kim, J. P. Lemmon, V. L. Sprenkle and Z. Yang, *Energy Environ. Sci.,* 2013, **6**, 299.
17. D. Peramunage and S Licht, *Science*, 1993, **261**, 1029.
18. R. Demir-Cakan, M. Morcerette, Gangulbabu, A. Gueguen, R. Dedryvere and J. Tarascon, *Energy Environ. Sci.,* 2013, **6**, 176.
19. S. Licht and H. Wu, *J. Phys. Chem. C.*, 2011, **115**, 25138.
20. S. Licht and B. Wang, *J. Phys. Chem. Lett.*, 2010, **1**, 2363.
21. S. Licht, *Advanced Materials,* 2011, **27,** 2993.